https://doi.org/10.5194/egusphere-2026-4006
Preprint. Discussion started: 21 July 2026

Selection of onset of acceleration points and failure time prediction of landslides based on ground-based radar

Hui Wu[a,b], Pingping Huang[a,b,c*], Weixian Tan[b,c], Yaolong Qi[b,c], Wei Xu[b,c], Yuejuan Chen[b,c]

a School of Mechanics and Aeronautics, Inner Mongolia University of Technology, Hohhot 010051, China.

b Inner Mongolia Key Laboratory of Radar Technology and Application, Hohhot 010051, China.

c College of Information Engineering, Inner Mongolia University of Technology, Hohhot 010051, China.

* Corresponding author

Prof. Pingping Huang, College of Science, Inner Mongolia University of Technology, Hohhot, 010051, China.

E-mail address: hwangpp@imut.edu.cn

Abstract: The inverse velocity method (INV) based on the onset of acceleration (OOA) point is widely used in landslide time prediction. However, the selection of OOA point affects the accuracy of INV prediction results. This study proposed a deformation standard deviation-OOA (DSD-OOA) point identification method based on the statistical characteristics of ground-based radar landslide area deformation data. By introducing a controllable variable, a modified INV method was derived. The OOA point identified by DSD-OOA was substituted into the modified INV method for landslide time prediction and compared with the prediction results of the moving average-OOA (MA-OOA) point method. Results show that compared to MA-OOA, the inverse velocity time series after the OOA point identified by DSD-OOA exhibits

https://doi.org/10.5194/egusphere-2026-4006
Preprint. Discussion started: 21 July 2026

smaller fluctuations and is closer to linear change. The INV predictions using MA-OOA (MA-OOA-INV) consistently lag behind the actual landslide time, while the INV predictions using DSD-OOA (DSD-OOA-INV) are more stable and consistently precede the actual landslide time of failure. Furthermore, the root mean square error (*RMSE*) and coefficient of determination (R^2) indicate that the DSD-OOA-INV method predicts landslide lifetime with higher accuracy, suggesting that OOA points identified by the DSD-OOA method can more precisely predict landslide time of failure.

Keywords: Onset of Acceleration; Landslide; Time Prediction; Ground-Based Radar

1 Introduction

Landslides are among the most common geological hazards, posing severe threats to human life and property (Abuda et al., 2026; Dille et al., 2026; Nava et al., 2026). Over the past few years, the expansion of China's mining sector has driven year-on-year growth in both the quantity and dimensions of open-pit operations, contributing to increasingly frequent landslides at mine sites (Jia et al., 2023; Wang et al., 2024). Given the necessity to ensure the safe evacuation of on-site personnel and equipment during mining landslides, the prediction of landslide failure time is of paramount importance (Intrieri et al., 2012; Szczepanek et al., 2024). To address this, ground-based radar has been widely applied in mine monitoring due to its various advantages (Zhou et al., 2021; Tan et al., 2023). The deformation data obtained through this method enables effective analysis and prediction of slope deformation trends (Wu et al., 2025; Wu et al., 2026).

https://doi.org/10.5194/egusphere-2026-4006
Preprint. Discussion started: 21 July 2026

Since the 1960s, many researchers have investigated landslide forecasting through laboratory tests and field-based studies. Saito (1965) divided the landslide deformation process into three stages based on the creep theory. Dick et al. (2015) suggested that the linear fitting of INV versus time should use data after the OOA prior to slope failure. Carlà et al. (2017) proposed using the intersection point of short-term and long-term velocity moving averages as the OOA point, successfully applying it to the inverse velocity method. Building on Carlà et al.'s research, Bozzano et al. (2018) further discussed the effects of sampling frequency and onset of acceleration point on INV fitting, and proposed a new method for continuously updating INV analysis. Zhou et al. (2020) modified the traditional INV method, making it applicable for predicting landslide time when deformation velocity is decelerating during the pre-failure stage, and validated it using ground-based radar monitoring data. The INV method has become a widely used tool for landslide time prediction due to its simplicity and practicality. However, the INV method also has certain limitations. When using inverse velocity data following different OOA points for prediction, the results can vary significantly. Therefore, there is an urgent need to find an OOA point identification method suitable for improving INV.

In summary, this study proposed an onset of acceleration (OOA) point identification method suitable for improved inverse velocity method (INV) based on landslide surface deformation data obtained from ground-based radar. Firstly, this work introduced the process and principles of the modified inverse velocity method and OOA point identification method. Secondly, the applicability and stability of the

https://doi.org/10.5194/egusphere-2026-4006
Preprint. Discussion started: 21 July 2026

proposed method were verified using three open-pit mine landslide cases. Finally, the prediction accuracy of the deformation standard deviation-OOA (DSD-OOA) point method and the moving average-OOA (MA-OOA) point method was evaluated using statistical error analysis indexes.

2 Method

2.1 Modified inverse velocity method

In 1985, Japanese researcher Fukuzono (1985a, 1985b) simulated rainfall-induced landslides through large-scale indoor experiments and proposed the inverse velocity concept for predicting the time of slope failure. The inverse velocity method is based on creep theory and analyzes the relationship between the reciprocal of velocity ($1/v$) and time during the accelerating deformation stage of slope movement. When landslides enter the tertiary creep stage, plotting inverse velocity against time typically produces a linear trend that can be extrapolated to zero to predict the failure time. Based on this concept, Voight (1988) conducted theoretical analyses of pure shear processes and exponential creep processes under static loading, establishing a relationship between displacement acceleration and velocity:

$$\dot{V} = AV^{\alpha} \tag{1}$$

Where: A、 α is the fitting parameter, V is velocity, and $\dot{V}$ is acceleration.

When $\alpha > 1$, after integrating with respect to time, the equation becomes:

$$V = \left[A(\alpha-1)(t_f - t) + V_f^{(1-\alpha)}\right]^{\frac{1}{1-\alpha}} \tag{2}$$

Where: t is the monitoring time, t_f is the time of landslide occurrence, and V_f is the velocity at the time of landslide.

https://doi.org/10.5194/egusphere-2026-4006
Preprint. Discussion started: 21 July 2026

When a landslide occurs, the velocity is typically assumed to be infinite, and thus equation (2) can be simplified to:

$$\frac{1}{V}=\left[A(\alpha-1)(t_f-t)\right]^{\frac{1}{\alpha-1}} \tag{3}$$

According to the experimental results and studies of Voight (1989) and Rose (2007), α typically ranges between 1.5 and 2.2. When $1.5 < \alpha < 2$, the inverse velocity curve is concave; when $\alpha > 2$, the curve is convex; and when $\alpha = 2$, the curve is linear. Statistical analysis has shown that most landslide inverse velocity curves are linear, i.e., $\alpha = 2$. Therefore, Equation (3) can be simplified to:

$$\frac{1}{V}=A(t_f-t) \tag{4}$$

Based on Equation (4), assuming t equals t_0 (where t_0 is the acceleration initiation point) and letting V equal V_0 (where V_0 is the velocity at t_0), we can obtain:

$$\frac{1}{V_0}=A(t_f-t_0) \tag{5}$$

Dividing Equation (4) by Equation (5) and simplifying yields the modified inverse velocity method model, as shown in the following equation:

$$\frac{1}{V}=\frac{1}{V_0}\times\left(1+\frac{t_0-t}{t_f-t_0}\right) \tag{6}$$

Based on Equation (6), the landslide failure time could be calculated by fitting the inverse velocity-time scatter points. The modified inverse velocity method considered the influence of different onset of acceleration (OOA) points on landslide failure time prediction. Therefore, to accurately predict landslide failure time, it was crucial to study the applicability of different OOA point identification methods.

2.2 Selection of onset of acceleration point

Ground-based radar has been widely used in landslide time of failure prediction

https://doi.org/10.5194/egusphere-2026-4006
Preprint. Discussion started: 21 July 2026

due to its advantages of high precision, area monitoring, long-range capability, and high frequency (Mazzanti et al., 2015; Dick et al., 2015; Zhou et al., 2021). The principle is that the two-dimensional sequential complex images acquired by the radar contain amplitude and phase information of the monitored target. By comparing radar image data from two different times to obtain their phase differences, high-precision deformation information of the observed targets can be derived (Wang et al., 2022; Qi et al., 2020), as shown in Figure 1.

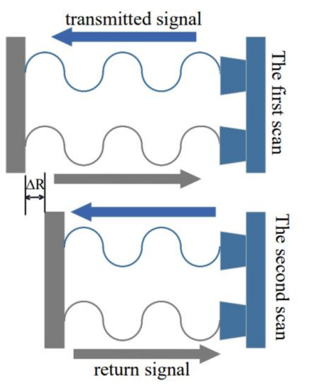

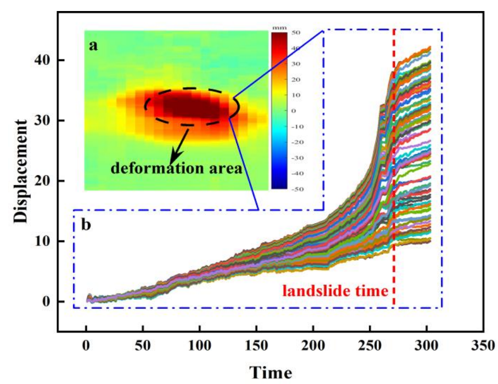

Fig. 1. Principle of deformation acquisition

Fig. 2. Landslide failure measurements captured by radar

When deformation occurs in the monitored slope, the radar deformation image effectively illustrates its pattern of change, as shown in Figure 2a. In the displacement map, the intensity of the colors corresponds to the magnitude of displacement, with green representing no deformation, blue indicating negative deformation, and darker red indicating larger positive displacements. The black oval delineates the primary deformation area where significant slope movement is concentrated. Each pixel in the deformation zone forms an independent cumulative deformation curve over time, as

https://doi.org/10.5194/egusphere-2026-4006
Preprint. Discussion started: 21 July 2026

shown in Figure 2b (due to the large number of pixels, Figure 2b only shows a portion of them). As observed in Figure 2b, when the slope is in stable creep deformation, the deformation values of all pixels fluctuate within a small range around a fixed value, approximating linear variation. However, when the slope undergoes accelerated deformation and approaches the time of landslide occurrence, the deformation values of all pixels exhibit greater fluctuation ranges at the same temporal instant, with the degree of dispersion in deformation values becoming increasingly significant. This phenomenon can be described using statistical theory, as shown in the following equation:

$$DSD = \sqrt{\frac{\sum_{i=1}^{n}(d_i - \bar{d})^2}{n-1}} \quad (7)$$

Where: DSD is standard deviation of displacement in the landslide area; d_i is displacement of different pixels at a given time; $\bar{d}$ is average displacement of different pixels at a given time; and n is the total number of pixel points at the same time.

The calculation results based on equation (7) are shown in Figure 3. As shown in Figure 3, the DSD-time curve integrates the variation patterns of all pixels in the landslide area and effectively describes the evolution process of landslide deformation. It demonstrates that during creep deformation, DSD increases almost linearly, while during accelerated deformation and approaching failure time, DSD increases sharply until after the landslide occurs. Based on the variation pattern of the DSD curve during the landslide deformation process, this work proposed a method for determining OOA points using DSD (referred to as the DSD-OOA method). This method involves piecewise linear fitting of the DSD-time curve, where the

https://doi.org/10.5194/egusphere-2026-4006
Preprint. Discussion started: 21 July 2026

intersection point of the two fitted lines represents the OOA point, as shown in Figure 4. The inverse velocity analysis starting from the obtained OOA point is termed the DSD-OOA-INV method.

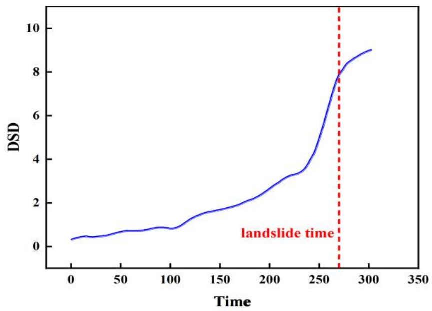

Fig. 3. DSD-time curve

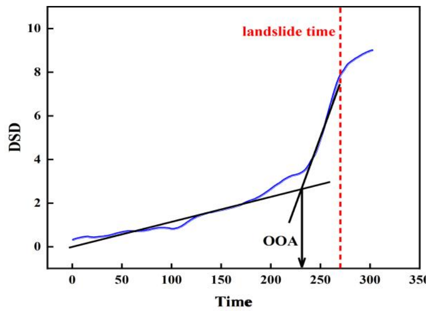

Fig. 4. Selection method of DSD-OOA point

Carlà et al. (2017) proposed a simple and innovative method for identifying the onset of acceleration points based on the intersection of short-term and long-term moving average velocity curves (abbreviated as MA-OOA method in this work). This method has been widely applied (Zhang et al., 2021), and the calculation process for long-term and short-term moving average velocities is as follows:

$$\bar{v} = \frac{v_t + v_{t-1} + \cdots v_{t-n+1}}{n} \tag{8}$$

Where: $\bar{v}$ is the moving average velocity; v is the velocity at time t; n is an integer multiple of the unit time, with n=3 typically used for short-term moving average velocity and n=7 for long-term moving average velocity.

Based on equation (8), the temporal variation curves of long-term and short-term moving average velocities were calculated, where their intersection point represents the OOA point (when the short-term moving average velocity curve is above the long-term moving average velocity curve), as shown in Figure 5. The inverse velocity

https://doi.org/10.5194/egusphere-2026-4006
Preprint. Discussion started: 21 July 2026

analysis starting from the identified OOA point is termed the MA-OOA-INV method.

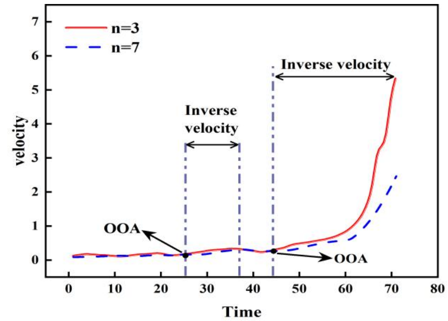

Fig. 5. Selection method of MA-OOA point

3 Case studies

3.1 Case Study 1: An open-pit coal mine

The mining area extends 3.3 kilometers east-west and 0.9 kilometers north-south, covering an area of 2.9 square kilometers. The altitude of the mining area ranges from 995.5 to 1,213.8 kilometers, with a relative height difference of 80 to 218.3 meters. The mine is mainly composed of grayish-white, grayish-black, and grayish-green sandstone, mudstone, and conglomerate. On June 18, 2024, a small landslide occurred due to the impact of construction vibrations, as shown in Figure 6.

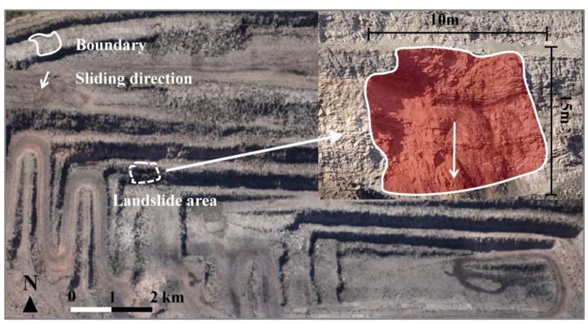

Fig. 6. Photographs of the mining area and landslide site

Around 12:00 on June 17, the standard deviation of deformation in this area

https://doi.org/10.5194/egusphere-2026-4006
Preprint. Discussion started: 21 July 2026

began to increase continuously, and the landslide occurred at 07:50 on June 18, as shown in Figure 7. The landslide had a relatively short duration but high displacement velocity. From initiation to failure, the velocity increased continuously, which is consistent with the classical creep theory model. Following the OOA identification methods described in section 2.2, we analyzed the inverse velocity time series after 21:09 on June 17 (MA-OOA method) and 01:31 on June 18 (DSD-OOA method), as shown in Figure 7 and 8. The inverse velocity showed an approximately linear distribution over time, with fitting coefficients of 0.801 and 0.873 for the MA-OOA and DSD-OOA methods, respectively.

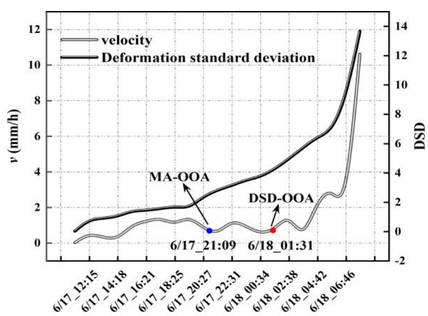

Fig. 7. DSD and velocity curves

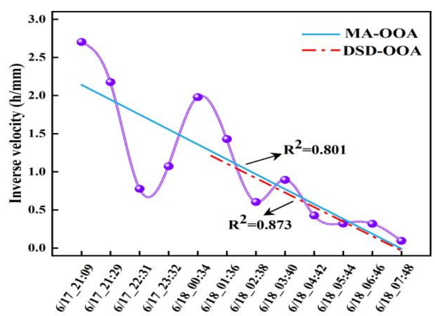

Fig. 8. Inverse velocity curves

Based on equation (6), we used the MA-OOA-INV and DSD-OOA-INV methods to fit inverse velocity scatter points and calculate the life expectancy of landslide, as shown in Figure 9. The life expectancy of landslide can be updated with the increase of data, which is an intuitive method to characterize the landslide time of failure. As shown in Figure 9, there are noticeable differences in the expected lifetime results calculated using the inverse velocity method based on OOA points obtained from MA and DSD approaches. The landslide time of failure predicted by the

https://doi.org/10.5194/egusphere-2026-4006
Preprint. Discussion started: 21 July 2026

MA-OOA-INV method show high fluctuation and significant errors, with a maximum error of 25.66%. Furthermore, the predicted failure time is mostly later than the actual landslide occurrence time. However, the landslide time curve predicted by the DSD-OOA-INV method approximately coincide with the actual landslide curve, with most predictions occurring before the actual failure time. As monitoring data increased, the prediction results of the DSD-OOA-INV method became increasingly closer to the actual failure time. The above analysis indicate that OOA points calculated from the DSD-time curve were more suitable for inverse velocity method predictions.

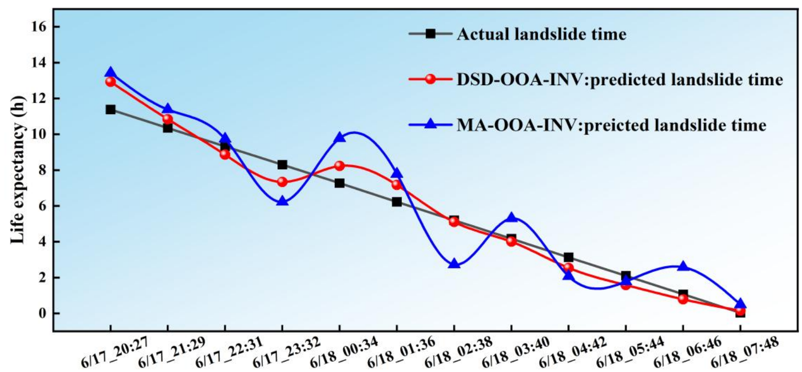

Fig. 9. The life expectancy of landslide

3.2 Case Study 2: An open-pit metal mine

The study site is a terraced open-pit metal mine in northwestern China, situated at elevations of approximately 1000~1300 m. The local strata are mainly composed of gneiss and other rocks. Prolonged excavation across the rugged terrain has created a series of mining benches (Figure 10a). On April 21, 2021, slope failure occurred following successive rainfall events, together with disturbances caused by long-term haulage activities (Figures 10a and 10b).

https://doi.org/10.5194/egusphere-2026-4006
Preprint. Discussion started: 21 July 2026

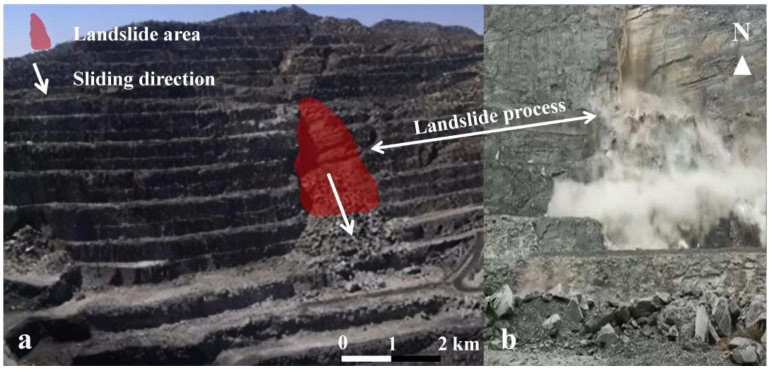

Fig. 10. Photographs of the mining area and landslide site

Figure 11 illustrates the deformation standard deviation and velocity evolution process of the landslide. As shown in Figure 11, prior to 19:20 on April 20, the deformation standard deviation exhibited near-linear growth while the velocity fluctuated around 0.2, indicating that the landslide was in a uniform deformation stage. Subsequently, the deformation standard deviation rose rapidly, accompanied by a sharp increase in velocity, culminating in the landslide occurrence at approximately 09:37 on April 21. The OOA points were identified using both MA-OOA and DSD-OOA methods, and their corresponding inverse velocity time series were analyzed, as presented in Figure 11 and 12. The results demonstrate that the inverse velocity time series following the OOA point identified by the DSD-OOA method exhibits a more pronounced linear trend, with a high fitting coefficient of 0.947. In contrast, the inverse velocity time series following the OOA point identified by the MA-OOA method shows greater fluctuations, yielding a lower fitting coefficient of 0.914.

https://doi.org/10.5194/egusphere-2026-4006
Preprint. Discussion started: 21 July 2026

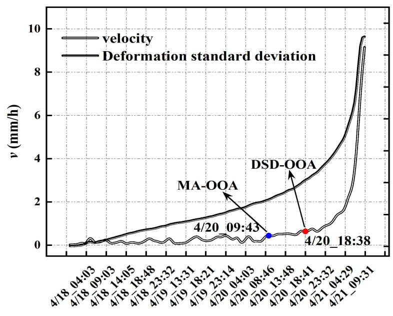

Fig. 11. DSD and velocity curves

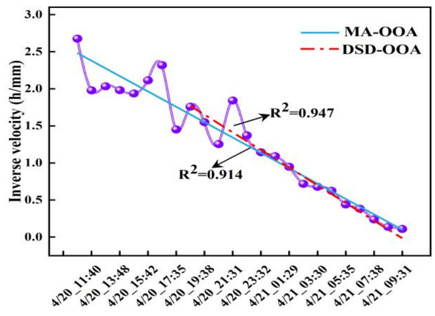

Fig. 12. Inverse velocity curves

The inverse velocity scatter points were fitted and the life expectancy of landslide was calculated using both MA-OOA-INV and DSD-OOA-INV methods, as illustrated in Figure 13. Figure 13 reveals that the MA-OOA-INV method yields predictions with considerable fluctuations. Although the predictions gradually approach the actual landslide time of failure as monitoring data accumulates, they consistently lag behind the actual occurrence time. In contrast, the DSD-OOA-INV method demonstrates that its expected slope lifetime curve closely aligns with the actual lifetime expectancy curve after the slope enters the acceleration stage, producing more stable predictions. With the increase of time series, the prediction time is closer to the actual landslide time of failure, and the prediction results are ahead of the actual landslide time of failure. Furthermore, the maximum error of predictions using the MA-OOA-INV method reaches 18.48%, whereas the DSD-OOA-INV method exhibits a significantly lower maximum error of only 8.39%. These analyses conclusively demonstrate that the DSD-OOA-INV method achieves superior predictive accuracy compared to the MA-OOA-INV method.

https://doi.org/10.5194/egusphere-2026-4006
Preprint. Discussion started: 21 July 2026

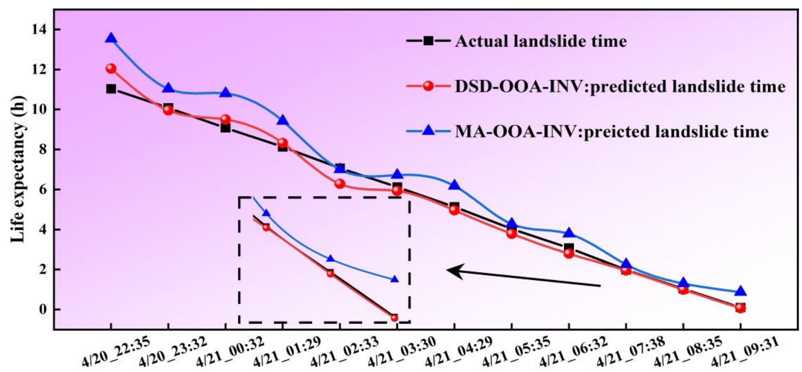

Fig. 13. The life expectancy of landslide

3.3 Case Study 3: An open-pit coal mine

The case study concerns a high-elevation open-pit coal mine in northwestern China (Figure 14a). The site lies between 1760 and 2025 m above sea level and occupies approximately 7.72 km^2 (Figure 14b). Its geological setting is characterized by a steep monocline, with strata striking 170° ~190° . The main rock type in the mining area is sandstone, and its compressive strength under saturated conditions ranges from 9.92 Mpa to 41.2 Mpa. On June 7, 2024, construction-induced vibrations triggered a slope failure at the mine (Figure 14c).

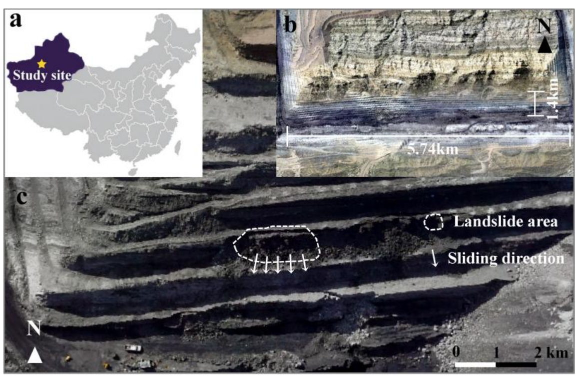

Fig. 14 Photographs of the mining area and landslide site

Figure 15 illustrates the evolution of deformation standard deviation and velocity

https://doi.org/10.5194/egusphere-2026-4006
Preprint. Discussion started: 21 July 2026

variations in the landslide. As evident from Figure 15, the deformation standard deviation can be divided into three distinct stages. In the first stage, the deformation standard deviation gradually increased, accompanied by distinct patterns in velocity changes, indicating slope displacement. Notably, at approximately 15:06 on the 6th, the displacement standard deviation increased rapidly, with velocity significantly rising to approximately 6 mm/h. Field inspection by personnel revealed the development of tension cracks at the slope's rear edge, as shown in Figure 16. During the second stage, the DSD increased gradually in an approximately linear manner, while velocity oscillated around a fixed value, reflecting uniform slope deformation. After the onset of acceleration, both the displacement standard deviation and velocity rose sharply, ultimately resulting in the landslide at 05:50 on the 7th.

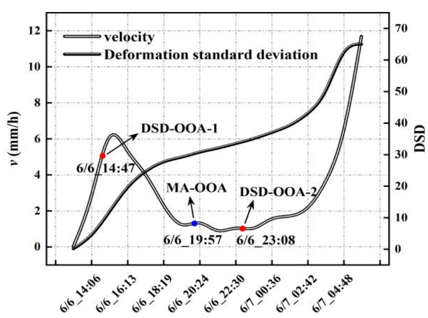

Fig. 15. DSD and velocity curves

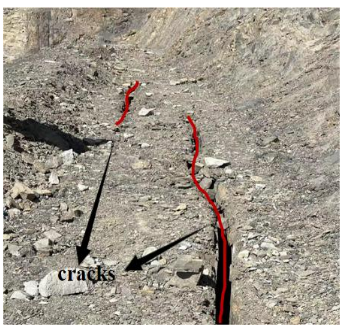

Fig. 16. The photo of site cracks

The OOA points were identified using the MA-OOA and DSD-OOA methods at 19:57 on the 6th, and at 14:47 and 23:08 on the 6th, respectively, as shown in Figure 15. Due to the brief increase in velocity after 14:47 (DSD-OOA-1) and then the continuous decline to a stable level, the inverse velocity did not show a linear trend tending towards 0. Therefore, the DSD-OOA-1 point will not be analyzed here and

https://doi.org/10.5194/egusphere-2026-4006
Preprint. Discussion started: 21 July 2026

will be discussed in detail in the method limitations section of the discussion part. The inverse velocity time series of the remaining two OOA points were analyzed, as shown in Figure 17. As shown in the figure, with increasing data points, the inverse velocity gradually approaches a linear trend following initial fluctuations. The OOA point identified by the DSD-OOA method is closer to the linear stage of the inverse velocity time series, achieving a high fitting coefficient of 0.983. In contrast, the inverse velocity time series following the OOA point identified by the MA-OOA method exhibits greater initial fluctuations before gradually transitioning to linear behavior, yielding a fitting coefficient of 0.941.

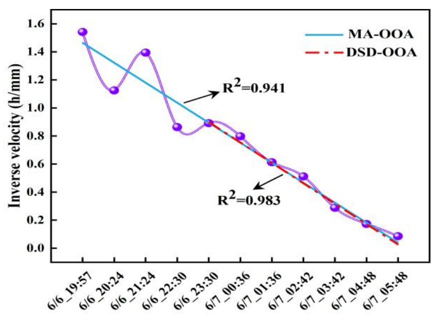

Fig. 17. Inverse velocity curves

The inverse velocity scatter points were fitted and the landslide lifetime was calculated using both MA-OOA-INV and DSD-OOA-INV methods, as illustrated in Figure 18. As shown in Figure 18, the MA-OOA-INV method exhibited significant fluctuations in its initial predictions. As monitoring data accumulated, the predicted landslide lifetime curve intersected with the actual lifetime curve at 23:25 on June 6, ultimately deviating from the actual landslide time of failure and demonstrating a lag effect in prediction performance. In contrast, the DSD-OOA-INV method produced

https://doi.org/10.5194/egusphere-2026-4006
Preprint. Discussion started: 21 July 2026

more stable predictions, with its landslide lifetime curve maintaining an approximately parallel relationship with the actual lifetime curve. As the time series expanded, after 23:30 on June 6, the expected lifetime curve showed both parallel convergence and overlapping convergence with the actual lifetime curve. However, it never fully coincided with the actual lifetime curve, demonstrating an early warning signal effect. Furthermore, the maximum prediction error of the MA-OOA-INV method was 18.71%, while the DSD-OOA-INV method achieved a lower maximum error of 10.07%.

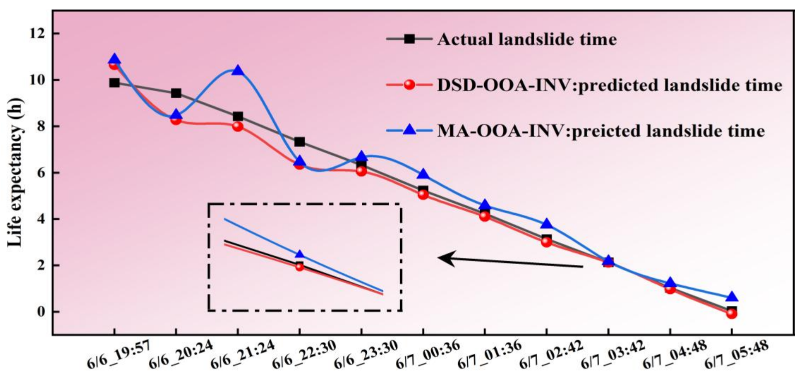

Fig. 18. The life expectancy of landslide

4 Discussion

4.1 Accuracy analysis of landslide lifetime prediction model

To further quantitatively evaluate the accuracy of landslide lifetime prediction models, statistical indexes were employed for analysis in this section. In statistics, common evaluation indexes for error estimation include root mean square error (*RMSE*), mean square error (*MSE*), mean absolute error (*MAE*), and coefficient of determination (R^2) (Roy et al., 2019; Qiu et al., 2024; Wang et al., 2026). *RMSE* addresses the issues of non-smoothness in *MAE* function and dimensional

https://doi.org/10.5194/egusphere-2026-4006
Preprint. Discussion started: 21 July 2026

inconsistency between *MSE* and original data, while R^2 serves as a normalized index that intuitively reflects the deviation between predicted and actual values. Therefore, *RMSE* and R^2 were selected as evaluation indexes for assessing prediction accuracy in this section.

The *RMSE* is defined as the square root of the ratio between the squared deviation of actual and predicted landslide lifetimes and the number of predictions, as shown in equation (9):

$$RMSE=\sqrt{\frac{1}{N}\sum_{i=1}^{N}(f(x)-t(x))^2} \tag{9}$$

Where: N is the number of predictions, $f(x)$ represents the actual landslide lifetime, and $t(x)$ denotes the predicted landslide lifetime.

The R^2 is calculated according to equation (10):

$$R^2=1-\frac{\sum_i (y_i-\overline{y}_i)^2}{\sum_i (\hat{y}_i-y_i)^2} \tag{10}$$

Where: y_i represents the actual landslide lifetime, $\overline{y}_i$ denotes the predicted landslide lifetime, and $\hat{y}_i$ is the arithmetic mean of actual landslide lifetimes.

In evaluating the prediction results, smaller *RMSE* values and R^2 values closer to 1 indicate higher prediction accuracy, as presented in Table 1.

Table 1 Results of *RMSE* and R^2

Case type and method		Method	
		RMSE	R^2
Case 1	DSD-OOA-INV	0.726	0.958
	MA-OOA-INV	1.568	0.806

Case 2	DSD-OOA-INV	0.417	0.985
	MA-OOA-INV	1.100	0.899
Case 3	DSD-OOA-INV	0.545	0.972
	MA-OOA-INV	0.843	0.932

As shown in Table 1, both prediction methods demonstrate relatively small *RMSE* values, indicating high prediction accuracy for both approaches. However, the *RMSE* values of the DSD-OOA-INV method were consistently lower than those of the MA-OOA-INV method, with minimum *RMSE* values of 0.417 and 0.843, respectively. Furthermore, the R^2 values of the DSD-OOA-INV method were consistently above 0.95 and higher than those of the MA-OOA-INV method. These analyses further demonstrate that the DSD-OOA-INV method achieves higher accuracy in landslide lifetime prediction, indicating that the OOA points identified by the DSD-OOA method are more suitable for the modified inverse velocity method than those identified by the MA-OOA method.

4.2 The limitations and applications of the DSD-OOA-INV method

The accuracy analysis presented above demonstrates that the DSD-OOA-INV method exhibits satisfactory prediction accuracy when valid OOA points are identified. However, the DSD-OOA method is also susceptible to false positives, as exemplified by the DSD-OOA-1 point illustrated in Figure 15. The inverse velocity analysis conducted using the velocity time series after this point is presented in Figure 19. As shown in the figure, the inverse velocity data during the DSD-OOA-INV-1 stage exhibit strong nonlinear characteristics, with the coefficient of determination (R^2)

https://doi.org/10.5194/egusphere-2026-4006
Preprint. Discussion started: 21 July 2026

of the fitted line being only 0.169, indicating an extremely poor linear fit. This suggests that the DSD-OOA-1 point is actually a false positive, where the deformation had not genuinely entered the accelerating stage at that moment, thereby precluding the establishment of a valid prediction model through inverse velocity analysis. In contrast, during the subsequent DSD-OOA-INV-2 stage, the inverse velocity data display a well-defined linear decreasing trend, with the R^2 of the fitted line reaching 0.983, indicating a remarkably high degree of linear correlation. This demonstrates that the DSD-OOA-2 point represents the truly valid OOA point, after which the deformation process conforms to accelerating creep characteristics, enabling reliable failure time prediction using the INV method. This comparison clearly illustrates that although the DSD-OOA method can identify potential onset points of acceleration, subsequent inverse velocity analysis is still required to verify their validity and eliminate false positive interference, thereby ensuring the reliability of prediction results.

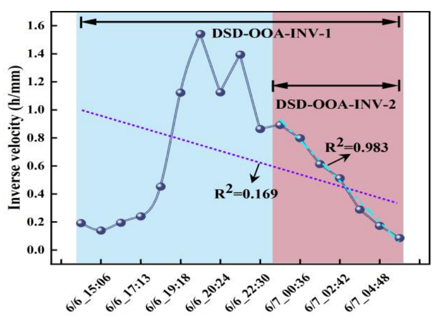

Fig. 19. Inverse velocity time series

The presence of false positives can lead to premature early warnings, potentially resulting in unnecessary resource waste. Therefore, in practical applications, it is essential to verify whether the identified OOA points are genuinely valid by incorporating the fitting performance of inverse velocity analysis (e.g., R^2 value), thereby enhancing the accuracy and reliability of early warnings. Moreover, false positive points typically manifest as short-term velocity spikes that subsequently stabilize or decline, failing to maintain a sustained acceleration trend. Based on these characteristics, the following measures are recommended for practical implementation. First, establish an R^2 threshold criterion, such as $R^2 \geq 0.6$, as the qualification condition for valid OOA points. Second, implement a dynamic updating mechanism for OOA points, whereby when an identified OOA point is verified as a false positive through inverse velocity analysis, the prediction process for that point should be immediately terminated, and the DSD-OOA algorithm should be reactivated to perform rolling identification on subsequent data to locate new valid OOA points. Third, adopt a tiered warning strategy, issuing an attention-level warning for initially identified OOA points, and upgrading to alert-level or danger-level warnings only after verification and confirmation, thus balancing the timeliness and accuracy of early warnings.

Although the DSD-OOA-INV method proposed in this study demonstrates promising application potential in slope failure early warning, several aspects warrant further investigation and refinement in future research. The current method primarily relies on R^2 thresholds and manual judgment to distinguish valid OOA points from false positives. Future work could incorporate machine learning or deep learning techniques to establish automated OOA point identification models, thereby

https://doi.org/10.5194/egusphere-2026-4006
Preprint. Discussion started: 21 July 2026

enhancing the intelligence level of the warning system. The existing method is predominantly based on displacement-velocity data from monitoring points. Future research should explore fusion identification techniques integrating multi-source heterogeneous data, such as rainfall, groundwater level, and acoustic emission, to reduce false positive risks from multiple dimensions. In addition, this study mainly focuses on slope instability prediction. Future work could attempt to extend the methodology to predictions in other domains, such as those dominated by quasi-brittle failure mechanisms and seismic event forecasting (Zhang et al., 2020; Niu et al., 2021; Riveros et al. 2026).

5 Conclusions

This work investigated the influence of different OOA point selection methods on inverse velocity prediction results based on ground-based radar data. Firstly, we derived and modified upon the traditional inverse velocity method. Secondly, the OOA point selection method was developed based on statistical patterns of radar data from landslide areas. Finally, the prediction accuracy and stability of DSD-OOA-INV and MA-OOA-INV methods were compared using three open-pit mine landslide cases. The main conclusions are as follows:

（1）The inverse velocity time series following the OOA point identified by the DSD-OOA method exhibits more linear behavior, whereas the inverse velocity time series following the OOA point identified by the MA-OOA method shows greater fluctuations.

（2）The MA-OOA-INV method yields predictions with significant fluctuations and consistently lags behind actual landslide occurrence times. In contrast, the DSD-OOA-INV method produces more stable predictions and consistently provides early warnings before actual landslide occurrences.

（3）Analysis of *RMSE* and R^2 demonstrates that the DSD-OOA-INV method achieves higher accuracy in landslide lifetime prediction, indicating that OOA points identified by the DSD-OOA method are more suitable for the modified INV method than those identified by the MA-OOA method. The modified INV method can improve the prediction accuracy by changing the selection of OOA points.

Data availability

The datasets supporting this study are available from the corresponding author upon reasonable request.

Author contributions

Hui Wu: Methodology, Writing-original draft. Pingping Huang: Conceptualization, Funding acquisition, Writing—review & editing. Weixian Tan: Resources, Funding acquisition, review & editing. Yaolong Qi: Validation. Wei Xu: Validation. Yuejuan Chen: Supervision.

Competing interests

The contact author has declared that none of the authors has any competing interests.

Acknowledgments

This study is supported in part by the Inner Mongolia Autonomous Region Science and Technology Program Project (Grant No. 2025KJTW0004), National Natural Science Foundation of China (Grant No. U25A20408), and Inner Mongolia

Autonomous Region Science and Technology Program Project (Grant No. 2025KYPT0128).

References

Abuda, J. B., Saturay, R. M., Catane, S. G., and Guevarra, I.: Lithologically-constrained, machine learning-based temporal landslide prediction models using rainfall time series for the Benguet First Engineering District, Philippines, Bull Eng Geol Environ, 85, 156, https://doi.org/10.1007/s10064-025-04764-4, 2026.

Bozzano, F., Mazzanti, P., and Moretto, S.: Discussion to: 'Guidelines on the use of inverse velocity method as a tool for setting alarm thresholds and forecasting landslides and structure collapses' by T. Carlà, E. Intrieri, F. Di Traglia, T. Nolesini, G. Gigli and N. Casagli, Landslides, 15, 1437–1441, https://doi.org/10.1007/s10346-018-0976-2, 2018.

Carlà, T., Intrieri, E., Di Traglia, F., Nolesini, T., Gigli, G., and Casagli, N.: Guidelines on the use of inverse velocity method as a tool for setting alarm thresholds and forecasting landslides and structure collapses, Landslides, 14, 517–534, https://doi.org/10.1007/s10346-016-0731-5, 2017.

Dille, A., Dewitte, O., Broeckx, J., Verbist, K., Sindiso Dube, A., Poesen, J., and Vanmaercke, M.: Capturing the complete landslide–debris-rich flood continuum for accurate inventory, susceptibility and exposure mapping – lessons from Cyclone Idai, Nat. Hazards Earth Syst. Sci., 26, 2561–2577, https://doi.org/10.5194/nhess-26-2561-2026, 2026.

https://doi.org/10.5194/egusphere-2026-4006
Preprint. Discussion started: 21 July 2026

Dick, G. J., Eberhardt, E., Cabrejo-Liévano, A. G., Stead, D., and Rose, N. D.: Development of an early-warning time-of-failure analysis methodology for open-pit mine slopes utilizing ground-based slope stability radar monitoring data, Can. Geotech. J., 52, 515–529, https://doi.org/10.1139/cgj-2014-0028, 2015.

Fukuzono T.: A Method to Predict the Time of Slope Failure Caused by Rainfall Using the Inverse Number of Velocity of Surface Displacement, Landslides, 22, 8-13_1, https://doi.org/10.3313/jls1964.22.2_8, 1985a.

Fukuzono T.: A new method for predicting the failure time of slope. Proceedings, 4th Int'l. Conference and Field Workshop on Landslides. 145-150, 1985b.

Intrieri, E., Gigli, G., Mugnai, F., Fanti, R., and Casagli, N.: Design and implementation of a landslide early warning system, Engineering Geology, 147–148, 124–136, https://doi.org/10.1016/j.enggeo.2012.07.017, 2012.

Jia, L., Wang, J., Gao, S., Fang, L., and Wang, D.: Landslide risk evaluation method of open-pit mine based on numerical simulation of large deformation of landslide, Sci Rep, 13, 15410, https://doi.org/10.1038/s41598-023-42736-4, 2023.

Mazzanti, P., Bozzano, F., Cipriani, I., and Prestininzi, A.: New insights into the temporal prediction of landslides by a terrestrial SAR interferometry monitoring case study, Landslides, 12, 55–68, https://doi.org/10.1007/s10346-014-0469-x, 2015.

Nava, L., Van Wyk De Vries, M., and Bell, L. E.: A workflow to identify and monitor slow-moving landslides through spaceborne optical feature tracking, Nat. Hazards Earth Syst. Sci., 26, 2305–2318, https://doi.org/10.5194/nhess-26-2305-2026, 2026.

Niu, Y. and Zhou, X.-P.: Forecast of time-of-instability in rocks under complex stress conditions using spatial precursory AE response rate, International Journal of Rock Mechanics and Mining Sciences, 147, 104908, https://doi.org/10.1016/j.ijrmms.2021.104908, 2021.

Qi, L., Tan, W., Huang, P., Xu, W., Qi, Y., and Zhang, M.: Landslide Prediction Method Based on a Ground-Based Micro-Deformation Monitoring Radar, Remote Sensing, 12, 1230, https://doi.org/10.3390/rs12081230, 2020.

Qiu, C. and Geng, X.: Travel distance estimation of landslide-induced debris flows by machine learning method in Nepal Himalaya after the Gorkha earthquake, Bull Eng Geol Environ, 83, 395, https://doi.org/10.1007/s10064-024-03883-8, 2024.

Rose, N. D. and Hungr, O.: Forecasting potential rock slope failure in open pit mines using the inverse-velocity method, International Journal of Rock Mechanics and Mining Sciences, 44, 308–320, https://doi.org/10.1016/j.ijrmms.2006.07.014, 2007.

Roy, J. and Saha, S.: Landslide susceptibility mapping using knowledge driven statistical models in Darjeeling District, West Bengal, India, Geoenviron Disasters, 6, 11, https://doi.org/10.1186/s40677-019-0126-8, 2019.

Riveros, A., Gunaratne, C., Martinelli, M., and Sperna Weiland, F. C.: A single framework for assessing flash flood and landslide susceptibility: an application to the Mediterranean Liguria region, Italy, Nat. Hazards Earth Syst. Sci., 26, 2437–2459, https://doi.org/10.5194/nhess-26-2437-2026, 2026.

https://doi.org/10.5194/egusphere-2026-4006
Preprint. Discussion started: 21 July 2026

Saito M.: Forecasting the time of occurrence of a slope failure. In: Proc 6th Int Conf soil mechanics and foundation eng, pp 537–541, 1965.

Szczepanek, R., Szczęch, M., and Kania, M.: Landslide type inference based on statistical analysis of a high-resolution digital elevation model in Gorce National Park, Poland, Sci Rep, 14, 14130, https://doi.org/10.1038/s41598-024-65026-z, 2024.

Tan, W., Wang, Y., Huang, P., Qi, Y., Xu, W., Li, C., and Chen, Y.: A Method for Predicting Landslides Based on Micro-Deformation Monitoring Radar Data, Remote Sensing, 15, 826, https://doi.org/10.3390/rs15030826, 2023.

Voight, B.: A method for prediction of volcanic eruptions. Nature, 332:125-130, 1988.

Voight, B.: A Relation to Describe Rate-Dependent Material Failure, Science, New Series, 243, 200–203, 1989.

Wang, H., Xu, L., Yu, H., and Zhang, J.: Research on prediction of high energy microseismic events in rock burst mines based on BP neural network, Sci Rep, 14, 29934, https://doi.org/10.1038/s41598-024-81614-5, 2024.

Wu, H., Huang, P., Tan, W., Qi, Y., Xu, W., and Chen, Y.: A new early warning method for landslide critical sliding tangent angle based on modified Nishihara model, Engineering Geology, 356, 108283, https://doi.org/10.1016/j.enggeo.2025.108283, 2025.

Wu, H., Huang, P., Tan, W., Qi, Y., Xu, W., and Chen, Y.: A generalized phenomenological method for extracting and warning of landslide deformation based on ground-based radar, Reliability Engineering & System Safety, 277,

https://doi.org/10.5194/egusphere-2026-4006
Preprint. Discussion started: 21 July 2026

113146, https://doi.org/10.1016/j.ress.2026.113146, 2026.

Wang, Z., Hu, J., Chen, Y., Liu, X., Liu, J., Wu, W., and Wang, Y.: Integration of ground-based and space-borne radar observations for three-dimensional deformations reconstruction: application to Luanchuan mining area, China, Geomatics, Natural Hazards and Risk, 13, 2819–2839, https://doi.org/10.1080/19475705.2022.2134828, 2022.

Wang, K., Xie, L., Xie, S., Zhang, S., Jiang, Y., Zhang, J., Zhu, L., Wang, Z., and Qi, F.: Constructing physical-based rainfall landslides prediction model: insights from rainfall threshold curves database of slope units, Nat. Hazards Earth Syst. Sci., 26, 2367–2385, https://doi.org/10.5194/nhess-26-2367-2026, 2026.

Zhang, J. and Zhou, X.: Forecasting Catastrophic Rupture in Brittle Rocks Using Precursory AE Time Series, JGR Solid Earth, 125, e2019JB019276, https://doi.org/10.1029/2019JB019276, 2020.

Zhang, Y., Ma, H., and Yu, Z.: Application of the method for prediction of the failure location and time based on monitoring of a slope using synthetic aperture radar, Environ Earth Sci, 80, 706, https://doi.org/10.1007/s12665-021-09989-6, 2021.

Zhou, X. and Ye, T.: Inverse-square-root-acceleration method for predicting the failure time of landslides, Sci. China Technol. Sci., 64, 1127–1136, https://doi.org/10.1007/s11431-020-1722-2, 2021.

Zhou, X.-P., Liu, L.-J., and Xu, C.: A modified inverse-velocity method for predicting the failure time of landslides, Engineering Geology, 268, 105521, https://doi.org/10.1016/j.enggeo.2020.105521, 2020.